Reaction Kinetics, Mechanisms and Catalysis (2023) 136:1933–1943
https://doi.org/10.1007/s11144-023-02456-2

Density functional theory study of N_2O decomposition catalyzed by $Pd_4^{-/0/+}$ clusters

Xinlin Tang[1] · Wenhong Zeng[1] · Huiyuan Duan[1] · Shuangkou Chen[1] · Xin Lian[1]

Received: 9 July 2023 / Accepted: 23 July 2023 / Published online: 27 July 2023

Abstract

Density functional theory (DFT) is used to investigate the N_2O decomposition over $Pd_4^{-/0/+}$ clusters. The Eley–Rideal (ER) mechanism and the Langmuir–Hinshelwood (LH) mechanism are well established. The average binding energies show that the most stable structure of $Pd_4^{-/0/+}$ clusters is the tetrahedral configuration. For the Pd_4^- cluster, the activation energies indicate that the rate-limiting step in two mechanisms is the formation of O_2, and the ER mechanism occurs more easily than the LH mechanism. While for the Pd_4^0 and Pd_4^+ clusters, the rate-limiting step in two mechanisms is the N_2O decomposition to N_2, and the LH mechanism is more likely to process. Among all clusters, the Pd_4^- cluster exhibits better catalytic activity compared with the Pd_4^0 and Pd_4^+ clusters.

Keywords DFT · Pd cluster · N_2O decomposition · Charge-state clusters

Introduction

N_2O, as a greenhouse gas, not only severely damages the ozone layer in the atmosphere, but also has a higher warming potential than CO_2 and CH_4 [1–3]. Recently, Shakoor et al. reported that the emission of N_2O is increasing due to anthropogenic activities [4]. Therefore, the elimination of N_2O has become one of the measures to mitigate atmospheric pollution. Among the N_2O treatment technologies, the direct catalytic decomposition of N_2O into N_2 and O_2 is regarded as the most promising method. There are mainly three main steps for the N_2O decomposition [5, 6]:

$$[\mathrm{Cat}] + N_2O \rightarrow N_2 + [\mathrm{Cat}]O^* \quad (1)$$

✉ Xin Lian
daisylian0121@163.com

[1] College of Chemistry and Chemical Engineering, Chongqing University of Science and Technology, Chongqing 401331, People's Republic of China

$$N_2O + [Cat]O^* \rightarrow [Cat] + N_2 + O_2\,(ER) \quad (2)$$

$$2[Cat]\,O^* \rightarrow [Cat] + O_2\,(LH) \quad (3)$$

The ER mechanism consists of the decomposition of two N_2O molecules. The first N_2O adsorbs on the catalyst and furtherly decomposes to N_2 and residual O^*. Then, the residual O^* binds to another N_2O to transform into N_2 and O_2. However, some researchers find that the residual O^* may react with another remaining O^* to further form O_2, which is known as the LH mechanism.

Small clusters are considered to be intermediates between the single atom and condensed matter. Many investigations have revealed that the reactivity of a cluster is dependent on the charge state. Francisco et al. [7] studied the charge effect on the N_2O reduction by the Rh_6^- and Rh_6^+ clusters, they found that the N_2O reduction process is influenced by the chosen charge of Rh particles. The Rh_6^- cluster has better catalytic activity compared with the Rh_6^+ cluster according to the activation energy results. Wu et al. [8] investigated the reaction mechanism of N_2O decomposition on $Au_3^{+/0/-}$ clusters, they point out that the Au_3 neutral cluster exhibited the highest catalytic activity, which just needs an energy barrier of 11.60 kcal/mol in the decomposition of N_2O. Lian et al. [9] explored the dissociation of water on neutral and charge-state Ni_3M (M = Ni, Cr, Mn, Fe, and Co) clusters. The results indicate that the dissociation barriers of anionic clusters are relatively low, and the bimetallic Ni_3Fe cluster exhibits the best performance.

Palladium catalysts have exhibited superior catalytic activity in many fields, especially in the control of automobile exhaust gas emissions [10, 11]. Its atoms, clusters, and compounds have been proven to be effective catalysts for N_2O decomposition [12–16]. However, the charge state influence of Pd nanoparticles on the catalytic activity is uncertain, and there is lack of theoretical study for the catalytic mechanism in the dissociation of N_2O on the charged Pd cluster.

Hence, in this work, the decomposition of N_2O on the $Pd_4^{+/0/-}$cluster has been investigated by DFT calculation. Two reaction mechanisms for N_2O decomposition on the $Pd_4^{+/0/-}$ cluster have been well established. For two mechanisms, the effects of the charge state on catalytic activity are elaborated. The results obtained can provide some theoretical guidance for solving the N_2O pollutant problem.

Computational methods

All DFT calculations were performed by Gaussian09 package [17]. The exchange–correlation interactions were treated by generalized gradient approximation (GGA) with Perdew-Burke-Ernzerhof (PBE) functional [18, 19]. The initial cluster structure optimization was performed at PBE/SDD level and the single point energy was calculated at PBE0/SDD level. The 6-311 + G(d,p) basis set was used for N and O atoms [20] and the SDD basis set was used for Pd atom [21]. The frequency analysis was supplemented by the same theoretical level to ensure that each TS has only one imaginary frequency.

The adsorption energy between cluster and molecules was calculated by Eq. 4:

$$E_{ads} = E_{system} - E_{cluster} - E_{molecule} \quad (4)$$

Here the E_{system} was the energy of the molecule adsorbed on the cluster, the $E_{cluster}$ was the energy of the cluster and the $E_{molecule}$ was the energy of the molecule.

Results and discussions

Adsorption of N_2O over the $Pd_4^{-/0/+}$ clusters

The overall possible configurations of $Pd_4^{-/0/+}$ clusters are optimized in various spin multiplicities, and the optimized structures are shown in Table S1. In all configurations of $Pd_4^{-/0/+}$ clusters, the tetrahedral structure is more stable and has higher binding energy than other configurations. Fig. S1 shows the most stable tetrahedral configuration of $Pd_4^{-/0/+}$ clusters. The Pd_4^{+} cluster is a regular tetrahedral configuration with an average bonding length of 2.59 Å and binding angle of 60°, the Pd_4^{0} and Pd_4^{-} clusters are slightly distorted tetrahedral structures with average binding lengths of 2.61 Å and 2.66 Å. This is consistent with the theoretical data of 2.66 Å for the Pd_4^{0} cluster reported by Camacho [22].

Then the N-terminal and O-terminal adsorption of N_2O at each possible site of $Pd_4^{-/0/+}$ clusters with various spin multiplicities are investigated, the full data are listed in Table S2. The adsorption energy is little affected by the different adsorption sites while it can be influenced availably by the adsorption pathway of N_2O. The adsorption energy, bond lengths between the $Pd_4^{-/0/+}$ clusters and N_2O in the N- and O-terminal adsorption are shown in Table 1. The adsorption energy of N_2O on the Pd_4^{-} cluster in N-terminal adsorption mode is the highest among the three clusters. Generally, the adsorption energy in the N-terminal adsorption pathway of N_2O is larger than that of the O-terminal, which suggests that the N_2O prefers to adsorb on the cluster through the N-terminal.

Mechanisms of N_2O decomposition on the $Pd_4^{-/0/+}$ clusters

Considering the potential energy profiles and the structures along the dissociation pathways are very similar, the reaction pathways of the N-terminal adsorption over

Table 1 The adsorption energy and the binding length between $Pd_4^{-/0/+}$ clusters and N_2O

	$Pd_4^{-/0/+}+N_2O$					
	$Pd_4^{-/0/+}-N_2O$			$Pd_4^{-/0/+}-ON_2$		
	E_{ads} (eV)	d_{Pd-N}(Å)	d_{N-O}(Å)	E_{ads} (eV)	d_{Pd-O}(Å)	d_{N-O}(Å)
Pd_4^{0}	− 0.55	2.07	1.18	− 0.28	2.42	1.18
Pd_4^{+}	− 0.60	2.17	1.16	− 0.41	2.34	1.19
Pd_4^{-}	− 1.03	1.94	1.21	− 0.24	2.31	1.18

$Pd_4^{-/0/+}$ clusters are mainly described in detail as shown in Figs. 1, 2, 3. The potential energy profiles in the O-terminal adsorption are shown in Figs. S2–S4.

For the N_2O reduction reaction, the initial step is the first N_2O decomposition. Fig. 1 shows the potential energy profiles of the first N_2O decomposition. For the Pd_4^- cluster, the first decomposition of N_2O needs two reaction processes to realize, while Pd_4^0 and Pd_4^+ clusters need just one step. For Pd_4^0 and Pd_4^+ clusters, the N_2O is slantly attached to the metal clusters with an ∠N–N–O angle of 180°, the energy of IM1* and IM** is − 0.52 eV and − 0.60 eV, respectively. Then, the

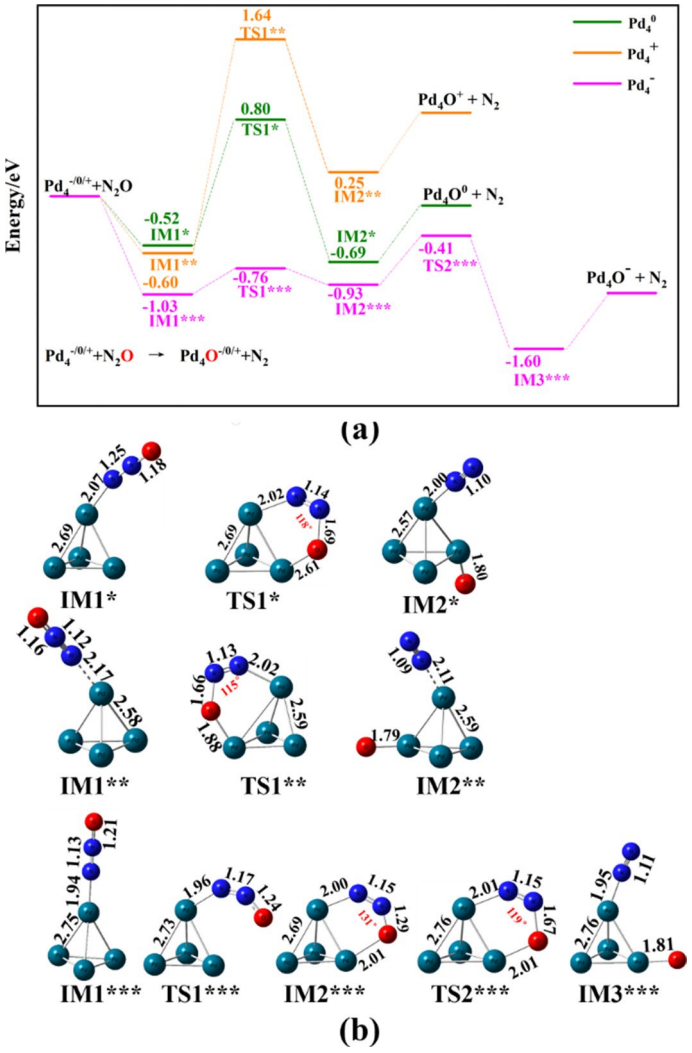

Fig. 1 The potential energy profile of the first N_2O decomposition on $Pd_4^{-/0/+}$ clusters of the N-terminal pathway **a** $N_2O \rightarrow N_2 + O^*$, and **b** corresponding optimized intermediates and transition states involved in N_2O decomposition

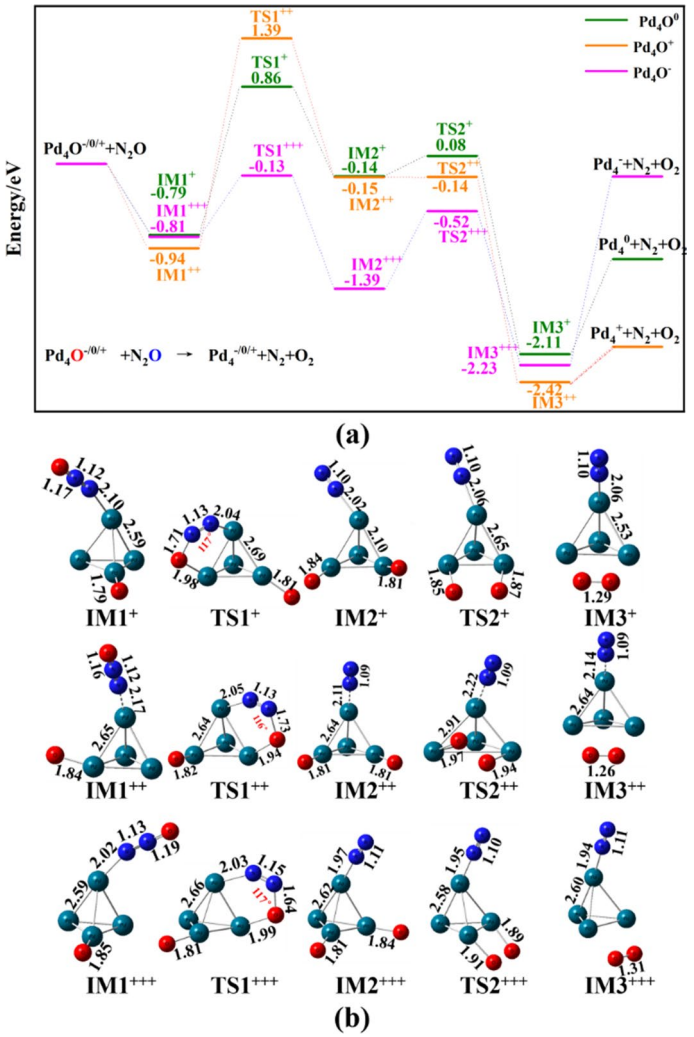

Fig. 2 The potential energy profile of ER mechanism in the N-terminal pathway **a** $O^* + N_2O \rightarrow N_2 + O_2$, and **b** corresponding optimized intermediates and transition states involved in ER mechanism

IM1* and IM1** convert to the IM2* and IM2** through transition states of TS1* and TS1**. The angle of ∠N–N–O is bent from the original 180–118° and 115°. The Pd–O bond with lengths of 1.98 Å and 1.88 Å. Subsequently, the O–N_2 bond is broken to form the N_2 molecule, and the dissociated O atom locates at the two adjacent Pd atoms of Pd_4^0 and Pd_4^+ clusters. The activation energies of this process are 1.32 eV and 2.24 eV.

For the Pd_4^- cluster, the N_2O molecule is vertically adsorbed on the metal cluster to form IM1*** with an adsorption energy of − 1.03 eV. Then, the IM1*** transfers to IM2*** through a transition state of TS1*** with an activation energy of 0.27 eV.

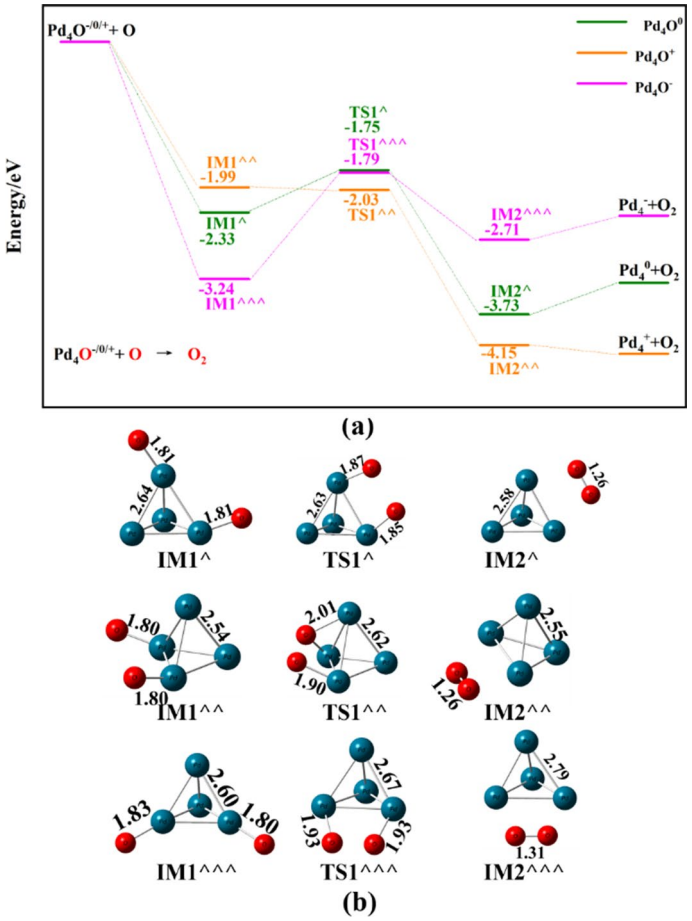

Fig. 3 The potential energy profile of LH mechanism in the N-terminal pathway **a** $2O^* \rightarrow O_2$, and **b** corresponding optimized intermediates and transition states involved in LH mechanism

The ∠N–N–O angle of N_2O is bent from 180 to 131° and the N and O atoms of N_2O are connected to neighboring Pd atoms. The N–O bond lengthens from 1.29 to 1.67 Å and finally breaks. The activation energy of this process is 0.52 eV.

The potential energy profiles of ER mechanism are shown in Fig. 2, the Pd_4O^0, Pd_4O^+, and Pd_4O^- clusters combine with another N_2O to further form $IM1^+$, $IM1^{++}$, and $IM1^{+++}$ with energies of − 0.79 eV, − 0.94 eV, and − 0.81 eV. Then, $IM1^+$, $IM1^{++}$, and $IM1^{+++}$ convert to $IM2^+$, $IM2^{++}$, and $IM2^{+++}$ through transition states of $TS1^+$, $TS1^{++}$, $TS1^{+++}$ with activation energies of 1.65 eV, 2.33 eV, and 0.68 eV. At this time, the N–O bond is broken and remains an O atom connecting to the $Pd_4O^{-/0/+}$ clusters. Finally, the two O atoms move close to each other by the lengthening of the Pd–O bond and generate the O_2 ($IM3^+$, $IM3^{++}$, and $IM3^{+++}$). The activation energies for this process are 0.22 eV, 0.01 eV, and 0.87 eV. Therefore, for the Pd_4O^0 and Pd_4O^+ clusters, the activation energy for the N_2O decomposition to N_2 is

higher than the O_2 formation, which indicates that the N_2O decomposition to N_2 is the rate-limiting step for the Pd_4O^0 and Pd_4O^+ clusters in the ER mechanism. However, for the Pd_4O^- cluster, the activation energy in the formation of O_2 is higher than the N_2O decomposition to N_2, implying that the formation of O_2 is the rate-limiting step.

The potential energy profiles of the LH mechanism are shown in Fig. 3. Different from the ER mechanism, the formation of O_2 in the LH mechanism is mainly from the recombination of two residual O atoms. As shown in Fig. 3, the Pd_4O^0, Pd_4O^+, and Pd_4O^- clusters combine with another O atom to form IM1^, IM1^^, and IM1^^^ with energies of − 2.33 eV, − 1.99 eV, and − 3.24 eV. Then, the IM1^, IM1^^, IM1^^^ to further form IM2^, IM2^^, IM2^^^ through transition states TS1^, TS1^^, TS1^^^. The activation energies of this process are 0.58 eV, − 0.04 eV, and 1.45 eV, which indicates that the Pd_4^+ cluster has the best catalytic activity for the formation of O_2 in LH mechanism. By comparing the ER mechanism and LH mechanism, it can be concluded that in the ER mechanism, the Pd_4^0 cluster and the Pd_4^+ cluster tend to form O_2, while the Pd_4^- cluster prefers to generate N_2.

To further understand the effect of the charge state for the Pd_4 clusters on the catalytic activity, we summarized all reaction energy barriers in Fig. 4. It is found that the charge state has significant effect on the catalytic activity. Among all investigated clusters, the Pd_4^- cluster exhibits superior catalytic activity for N_2O decomposition, just needing 0.52 eV (the first N_2O decomposition) and 0.68 eV (the second N_2O decomposition) of the N-terminal pathway. It is much lower than the reported data of $Au_{19}Pd$ (1.12 eV) [23] and PdC_{23} (1.45 eV, 2.97 eV) [24] clusters. The Pd_4^+ cluster shows excellent catalytic activity for the O_2 formation, which does not even need activation energy in the N-terminal pathway. As for the two mechanisms, it is noted that most of reactions are thermodynamically favorable. Furthermore, for the Pd_4^- cluster, the rate-limiting step is the formation of O_2, while the decomposition of N_2O to N_2 is the rate-limiting step for the Pd_4^0 and the Pd_4^+ clusters. Additionally, the energy barrier for the rate-limiting step in the LH mechanism is lower than the ER mechanism, which indicates the LH mechanism is more favorable.

Mulliken atomic charge analysis

The reactivity of the metal clusters derives from their electronic structure, thus we use the Mulliken atomic charge analysis to make a detailed investigation of the charge distribution between $Pd_4^{-/0/+}$ clusters and N_2O. The Mulliken charges of N- and O-terminal for N_2O molecule adsorbs on $Pd_4^{-/0/+}$ clusters as shown in Table 2. Electrons transfer from $Pd_4^{-/0/+}$ clusters to N_2O, suggesting that the $Pd_4^{-/0/+}$ clusters donate electrons to the N_2O as a Lewis base. Additionally, the Pd_4^- has the maximum amount of charge (1.425 e) transferred to the adsorbed N_2O, indicating the Pd_4^- cluster has strong attraction for N_2O molecule. This phenomenon is consistent with the results of the adsorption energies. By comparing the N_2O decomposition barriers with the amounts of charge transfer from clusters to N_2O, it is found that the more charge transfer, the lower dissociation barrier. This is due to the large number of electrons that accumulate on the N_2O molecule, making it easy to activate.

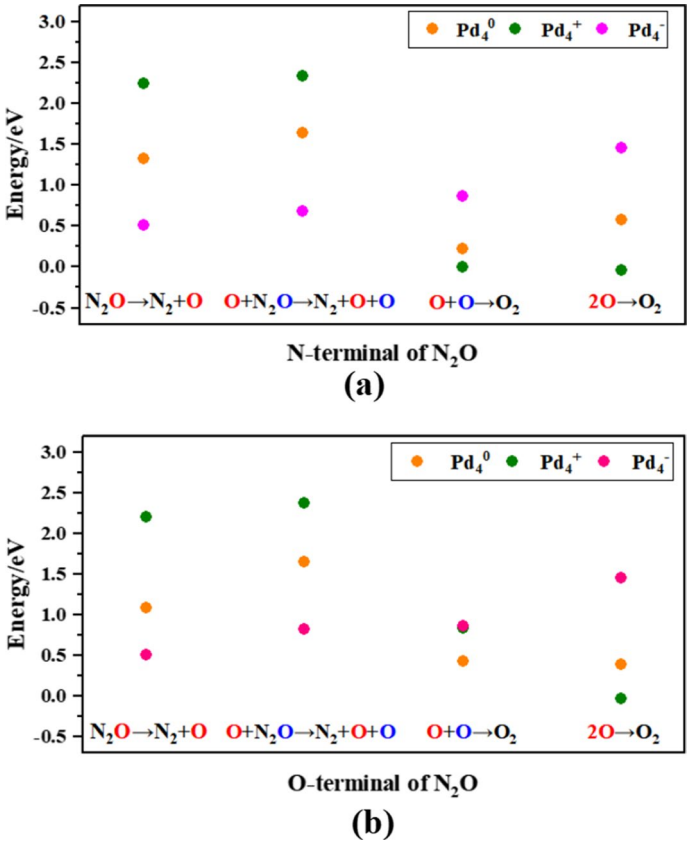

Fig. 4 The activation energy for the decomposition of N_2O on the $Pd_4^{-/0/+}$ clusters **a** the N- terminal pathway, and **b** the O- terminal pathway

Table 2 The amounts of Mulliken charge transferred from the metal clusters to the adsorbed N_2O

Cluster	Pd_4^0		Pd_4^+		Pd_4^-	
	$-N_2O$	$-ON_2$	$-N_2O$	$-ON_2$	$-N_2O$	$-ON_2$
Electron (e)	− 0.761	0.093	− 0.633	0.148	− 1.425	− 0.055

Therefore, of three different charged Pd clusters, Pd_4^- shows the best activity for N_2O decomposition.

Molecular orbital analysis

The reaction activity can be determined by the energy values of the HOMO and LUMO of a molecule, as well as their energy difference ΔE. The HOMO represents the highest energy level of occupied electrons in a molecule and exhibits a high electron-donating capability. The LUMO represents the lowest energy level

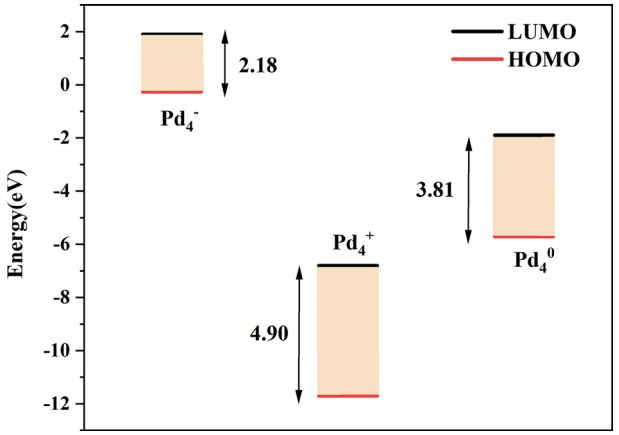

Fig. 5 HOMO and LUMO orbital energies of $Pd_4^{-/0/+}$ clusters, and the value of band gap (ΔE)

of unoccupied electrons in a molecule and possesses an electron-accepting ability. Thus, the smaller ΔE indicates that the electrons on the HOMO level are more likely to transfer to the LUMO level. The value of HOMO, LUMO and ΔE of $Pd_4^{-/0/+}$clusters are presented in Fig. 5. It can be observed that the HOMO value of Pd_4^- cluster is higher than Pd_4^+ and Pd_4^0 clusters, suggesting that Pd_4^- cluster has a better electron donation ability. The value of LUMO is $Pd_4^+ < Pd_4^0 < Pd_4^-$, which means that the Pd_4^+ cluster is prone to accepting electrons. The Pd_4^- cluster has the smallest difference (ΔE) of 2.18 eV. The small energy difference makes Pd_4^- easy to dissociate N_2O, which is consistent with results of the N_2O decomposition energy barrier.

Conclusion

The decomposition of N_2O on $Pd_4^{-/0/+}$ clusters has been investigated by DFT calculation. The adsorption energies show that the N_2O prefers to adsorb on Pd clusters through N-terminal than the O-terminal. The potential energy profiles show that the N- or O-terminal adsorption of N_2O has little influence on the decomposition barriers of N_2O. The Pd_4^- cluster exhibits excellent catalytic activity in the N_2O decomposition to N_2, which just needs 0.52 eV (the first N_2O decomposition) and 0.68 eV (the ER mechanism) in the N- terminal pathway. The Pd_4^+ cluster shows the best catalytic activity in the formation of O_2, and no activation energy is even required in the N-terminal pathway. Molecular orbital analysis indicates that the excellent catalytic activity of Pd_4^- cluster is due to the relatively small energy difference between the HOMO and LUMO. Besides, the Mulliken atomic charge analysis shows that the electron accumulation on the N_2O can increase the interaction between the N_2O molecule and $Pd_4^{-/0/+}$ clusters, and reduce the N_2O decomposition activation energy. These conclusions provide theoretical support for designing potential catalytic materials by regulating charge states.

Supplementary Information The online version contains supplementary material available at https://doi.org/10.1007/s11144-023-02456-2.

Acknowledgements This work is supported by the Science and Technology Research Program of Chongqing Municipal Education Commission (KJQN202101517).

Declarations

Conflict of interest The authors declare that they have no conflict of interest.

References

1. Itokawa H, Hanaki K, Matsuo T (2001) Nitrous oxide production in high-loading biological nitrogen removal process under low cod/n ratio condition. Water Res 35(3):657–664. https://doi.org/10.1016/S0043-1354(00)00309-2
2. Yan X, Zheng SK, Qiu DZ, Yang J, Han YP, Huo ZM, Su XF, Sun JH (2019) Characteristics of N_2O generation within the internal micro-environment of activated sludge flocs under different dissolved oxygen concentrations. Bioresour Technol 291:121867. https://doi.org/10.1016/j.biortech.2019.121867
3. Tian HQ et al (2020) A comprehensive quantification of global nitrous oxide sources and sinks. Nature 586:248–256. https://doi.org/10.1038/s41586-020-2780-0
4. Shakoor A et al (2021) Effect of animal manure, crop type, climate zone, and soil attributes on greenhouse gas emissions from agricultural soils-A global meta-analysis. J Clean Prod 278:124019. https://doi.org/10.1016/j.jclepro.2020.124019
5. Tanaka S, Yuzaki K, Ito S, Kameoka S, Kunimori K (2001) Mechanism of O_2 desorption during N_2O decomposition on an oxidized Rh/USY catalyst. J Catal 200(2):203–208. https://doi.org/10.1006/jcat.2001.3197
6. Yamashita T, Vannice A (1996) N_2O decomposition over manganese oxides. J Catal 161(1):254–262. https://doi.org/10.1006/jcat.1996.0183
7. Francisco H, Bertin V, Soto JR, Castro M (2016) Charge and geometrical effects on the catalytic N_2O reduction by Rh_6^- and Rh_6^+ clusters. J Phys Chem C 120(41):23648–23659. https://doi.org/10.1021/acs.jpcc.6b08172
8. Wu LY, Chen C, Luo L, Wang YC, Yin B (2020) DFT Study of the reaction mechanism of N_2O decomposition on $Au_3^{+/0/-}$ clusters. ChemistrySelect 5:5391–5399. https://doi.org/10.1002/slct.202000752
9. Lian X, Guo WL, Nie Y, Xu P, Yi H, He B, Chen SK (2019) A density functional study of water dissociation on small cationic, neutral, and anionic Ni-based alloy clusters. Chem Phys 521:44–50. https://doi.org/10.1016/j.chemphys.2019.01.019
10. Omrani M, Goriaux M, Liu Y, Martinet S, Jean-Soro L, Ruban V (2020) Platinum group elements study in automobile catalysts and exhaust gas samples. Environ Pollut 257:113477. https://doi.org/10.1016/j.envpol.2019.113477
11. Cao YD, Ran R, Wu XD, Si ZC, Kang FY, Weng D (2022) Progress on metal-support interactions in Pd-based catalysts for automobile emission control. J Environ Sci 125:401–426. https://doi.org/10.1016/j.jes.2022.01.011
12. Kim K, Baek S, Kim JJ, Han JW (2020) Catalytic decomposition of N_2O on Pd_xCu_y alloy catalysts: a density functional theory study. Appl Surf Sci 510:145349. https://doi.org/10.1016/j.apsusc.2020.145349
13. Xing W, Yang XF, Wang AQ, Li L, Liu XY, Zhang T, Mou CY, Li J (2012) Bimetallic Au-Pd alloy catalysts for N_2O dissociation: effects of surface structures on catalytic activity. J Phys Chem C 116(10):6222–6232. https://doi.org/10.1021/jp210555s
14. Kokalj A (2003) N_2O interaction with Pd(110): cluster vs. slab model. Surf Sci 532–535:213–220. https://doi.org/10.1016/S0039-6028(03)00460-6
15. Hintz PA, Ervin KM (1995) Chemisorption and oxidation reactions of nickel group cluster anions with N_2, O_2, CO_2, and N_2O. J Chem Phys 103(18):7897–7906. https://doi.org/10.1063/1.470207

16. Parres-Esclapez S, Illán-Gómez MJ, Lecea SMD, Bueno-López A (2010) On the importance of the catalyst redox properties in the N_2O decomposition over alumina and ceria supported Rh, Pd and Pt. Appl Catal B 96(3–4):370–378. https://doi.org/10.1016/j.apcatb.2010.02.034
17. Frisch MJ, Trucks GW, Schlegel HB, Scuseria GE, Robb MA, Cheeseman JR, Scalmani G, Barone V, Mennucci B, Petersson GA, Nakatsuji H, Caricato M, Li X, Hratchian HP, Izmaylov AF, Bloino J, Zheng G, Sonnenberg JL, Hada M, Ehara M, Toyota K, Fukuda R, Hasegawa J, Ishida M, Nakajima T, Honda Y, Kitao O, Nakai H, Vreven T, Montgomery JA Jr, Peralta JE, Ogliaro F, Bearpark M, Heyd JJ, Brothers E, Kudin KN, Staroverov VN, Keith T, Kobayashi R, Normand J, Raghavachari K, Rendell A, Burant JC, Iyengar SS, Tomasi J, Cossi M, Rega N, Millam JM, Klene M, Knox JE, Cross JB, Bakken V, Adamo C, Jaramillo J, Gomperts R, Stratmann RE, Yazyev O, Austin AJ, Cammi R, Pomelli C, Ochterski JW, Martin RL, Morokuma K, Zakrzewski VG, Voth GA, Salvador P, Dannenberg JJ, Dapprich S, Daniels AD, Farkas O, Foresman JB, Ortiz JV, Cioslowski J, Fox DJ (2010) Gaussian 09. Revision B.01.01. Gaussian Inc., Wallingford
18. Perdew JP, Chevary JA, Vosko SH, Jackson KA, Pederson MR, Singh DJ, Fiolhais C (1992) Atoms, molecules, solids, and surfaces: applications of the generalized gradient approximation for exchange and correlation. Phys Rev B 46(11):6671–6687. https://doi.org/10.1103/physrevb.46.6671
19 Perdew JP, Burke K, Ernzerhof M (1996) Generalized gradient approximation made simple. Phys Rev Lett 78:1396. https://doi.org/10.1103/PhysRevLett.77.3865
20. Curtiss LA, McGrath MP, Blaudeau JP, Davis NE, Binning RC, Radom L (1995) Extension of Gaussian-2 theory to molecules containing third-row atoms Ga-Kr. J Chem Phys 103:6104–6113. https://doi.org/10.1063/1.470438
21. Cao XY, Dolg M (2002) Segmented contraction scheme for small-core lanthanide pseudopotential basis sets. J Mol Struct (Thoechem) 581:139–147. https://doi.org/10.1016/j.theochem.2003.12.015
22. Camacho-Mendoza RL, Cruz-Borbolla J (2020) Reaction mechanism for hydrogen production using the Pd_4 cluster and formic acid by DFT. Chem Phys Lett 755:137794. https://doi.org/10.1016/j.cplett.2020.137794
23. Yu WL, Zuo HW, Lu CH, Li Y, Zhang YF, Chen WK (2015) Nitrous oxide decomposition catalyzed by $Au_{19}Pd$ and $Au_{19}Pt$ clusters. Acta Phys Chim Sin 31(3):425–434. https://doi.org/10.3866/PKU.WHXB201501191
24. Derdare M, Boudjahem AG, Boulbazine M (2022) Adsorption and decomposition mechanism of N_2O molecule over MC_{23} (M=Ru, Mn, V, Pd, and Rh) nanoclusters: a comparative DFT investigation. Struct Chem 33:2043–2062. https://doi.org/10.1007/s11224-022-01984-2